3D-imaging inspired improvements to hearing model in parasitoid fly *Ormia ochracea*

Max Mikel-Stites[a], Mary K. Salcedo[a], John J. Socha[a], Paul E. Marek[b], and Anne E. Staples[a]

[a]Engineering Mechanics Program, Department of Biomedical Engineering and Mechanics, Virginia Tech, Blacksburg, VA, 24061, USA; [b]Department of Entomology, Virginia Tech, Blacksburg, VA, 24061, USA

This manuscript was compiled on September 15, 2021

Although most binaural organisms localize sound sources using neurological structures to amplify the sounds they hear, some animals use mechanically coupled hearing organs to do so. One example, the parasitoid fly *Ormia ochracea*, has astoundingly accurate sound localization abilities and can locate objects in the azimuthal plane with a precision of $2°$, equal to that of humans. This is accomplished despite an intertympanal distance of only 1.2 mm, which is about $1/100$th of the wavelength of the sound emitted by the crickets that it parasitizes. In 1995, Miles *et al.* developed a model for hearing mechanics in *O. Ochracea*, which works well for incoming sound angles of less than $\pm 30°$, but suffers from reduced accuracy at higher angles. Despite this, it has served as the basis for multiple bio-inspired microphone designs for decades. Here, we present critical modifications to the classic *O. ochracea* hearing model based on information from 3D reconstructions of *O. ochracea*'s tympana. The 3D images reveal that the tympana have curved lateral faces in addition to the flat front-facing prosternal membranes represented in the 1995 model. To mimic these faces, we incorporated spatially-varying spring and damper coefficients that respond asymmetrically to incident sound waves, making a new quasi-two-dimensional (q2D) model. This q2D model has high accuracy (average errors of less than 10%) for the entire range of incoming sound angles. This improved biomechanical hearing model can inform the development of new technologies and may help to play a key role in developing improved hearing aids.

acoustics | hearing | biomechanics | mathematical modeling | sensory modeling | Ormia ochracea| parasitoidism | bioinspiration

The ability to localize sound allows animals to avoid predators and assist in finding and capturing prey. Binaural organisms, those with two ears, locate sound-emitting objects by comparing the intensity and timing of incident sound waves arriving at their two hearing organs (Fig. 1A). Sound localization is commonly described using two metrics: 1) interaural time delay (ITD), the difference in time it takes sound to reach the two hearing organs, and 2) interaurual amplitude difference (IAD), the difference in sound amplitude between the two organs (Fig. 1A) (1).

The particulars of sound localization are complex and vary widely among animals, as the ITD and IAD ranges experienced by binaural animals demonstrate (Fig. 1B) and the particular biophysics of sound localization for a specific animal are often too complex to be modeled well by simple analytical models. However, simplistic insect hearing models can be used to extract key principles of binaural hearing without complex physiological modeling of neural processes.

For the *tachinid* fly *Ormia ochracea*, the ability to hear its host cricket plays a key role in its reproductive cycle and overall fitness. As a parasitoid, *O. ochracea* listens to chirping male crickets and follows the sound back to the source, where female *O. ochracea* then deposit their larvae (2). Gravid *O. ochracea* females will remain in an area for extended periods of time in response to a cricket chirping, even if no cricket is present (3). Given its small size, if *O. ochracea* relied exclusively on the distance between its prosternal tympanal membranes (Fig. 1C), the ITD it experiences would be far too small to reliably localize sounds, and there would be no practical difference in IAD between the two membranes. To solve this scaling problem without resorting to bulky and complex neurological structures, *O. ochracea* females have two large mechanically coupled membranous tympana directly beneath their head (Fig. 1C). These coupled tympana are composed of a pair of prosternal membranes, joined together by an intertympanal bridge (4), with notable sexual dimorphism (Fig. 1C). This distinctive mechanical coupling serves to increase the ITD and IAD perceived by the fly, henceforth referred to as mITD (mechanical ITD) and mIAD (mechanical IAD), with these new increased mechanical values allowing it to localize chirping crickets. Since *O. ochracea* are active at or after dusk, they also use their hearing to avoid predation by bats, exhibiting a startle response while in flight to bat sonar frequency sound, similarly to preying mantises (5, 6). As such, the ability to accurately and quickly locate a source of incoming sound at high levels of lateral angular resolution is a significant advantage, es-

Significance Statement

In 1995 Miles *et al.* developed a mechanical model for hearing in the parasitoid fly *Ormia ochracea*, treating its highly three-dimensional (3D) tympanal membranes as flat plates. While this model has inspired significant research into *O. ochracea*-inspired directional microphone designs, it becomes increasingly inaccurate at high lateral angles and fails to include multiple realistic features present in O. ochracea physiology. Here, we performed 3D imaging of *O. ochracea* tympanal organs and used the morphological information to introduce variable coefficients into the 1995 model. These additions extended its accurate range from $\pm 30°$ to all incoming sound angles. Our modified model provides a new avenue for future studies related to *O. ochracea* and may lead to novel *O. ochracea*-inspired directional microphone designs.

Author contributions: M.M.S developed modification functions; M.M.S and A.E.S designed and wrote code; M.K.S and J.J.S performed 3D imaging and reconstruction work and processing; M.M.S. and A.E.S analyzed data and evaluated models; M.K.S made figures; P.M. performed photographic work; and M.M.S, M.K.S, P.M., J.J.S, and A.E.S wrote the paper.

The authors declare no conflict of interest. The funders had no role in the design of the study; in the collection, analyses, or interpretation of data; in the writing of the manuscript, or in the decision to publish the results.

[1]A.O.(Author One) contributed equally to this work with A.T. (Author Two) (remove if not applicable).

[2]E-mail: staplesa@vt.edu

DRAFT

pecially in potentially noisy environments (7), suggesting that *O. ochracea* may be a good source of bioinspiration to tackle the so-called cocktail party problem (8) (isolating sounds in a noisy environment) for directional microphones and hearing aids.

This small parasitoid fly may be an exception to the difficulty of accurately and simply modeling binaural hearing in a phonotactic animal (2) and has been the focus of numerous studies featuring its unique hearing organs and how they function (4, 5, 9–15). To investigate the biomechanical mechanisms that underlie *O. ochracea*'s unusual hearing abilities, Miles, Robert, and Hoy developed a mathematically tractable mechanical model of the ormiine's coupled tympana in 1995 (11). The authors validated their model against experimental data, recording tympanal membranes' positions and velocities, and consequently mIAD and mITD, as a function of the incident sound pressure, intensity, and angle. The 1995 model becomes analytically solvable under the assumptions of continuous sinusoidal input and symmetric model parameters, in addition to being numerically solvable without requiring the assumptions of symmetry or continuity. The model allowed Miles *et al.* to demonstrate that *O. ochracea*'s impressive sound localization abilities are due to the mechanical pre-processing performed by their mechanically coupled tympana, which mechanically amplify ITD and IAD experienced by the fly. Prior to our study, the original 1995 model was the only existing model for ICE (internally coupled ears)-based hearing in *ormiine* flies (16).

The model also accurately predicted mITD for all incoming sound angles and mIAD for angles below ±30° in a sample *O. ochracea* population and successfully provided a physiological explanation for *ochracea*'s localization prowess. Both the measured and predicted mITD indicated that *ochracea* possesses an mITD comparable to the ITD of an animal closer in size to a rat (Fig. 1 B). Later experiments successfully determined that *O. ochracea* had sound localization precision in the azimuthal plane of 2° (17, 18), a precision comparable to that of humans. The relative simplicity of the 1995 model and mechanical properties of the hearing structure used by *O. ochracea* has led to a new stream of research in *ochracea*-inspired designs for directional microphones and hearing aids (19–25).

The lumped element mechano-mathematical model designed by Miles *et al.* focused primarily on the dynamics of the intertympanal bridge and the front of the tympanal membranes (see Figure 1C). It models each membrane as a flat plate and gives a purely one-dimensional membrane amplitude response. The model spring and damper coefficients were adjusted until the model response approximated experimental responses in recently deceased *O. ochracea* (measured through laser vibrometry). Although the model is relatively accurate for mITD at most incident sound angles, it displays significant errors in mIAD for incident sound angles whose absolute value are larger than approximately ±30° from the midline of the fly and mITD becomes increasingly inaccurate at angles above approximately ±40°.

Previous scanning electron microscopy images of *O. ochracea* tympana had indicated that a certain degree of dynamic curvature and morphological complexity was present (4). It was excluded, however, primarily to avoid increasing model complexity. We hypothesized that inclusion of 3D features

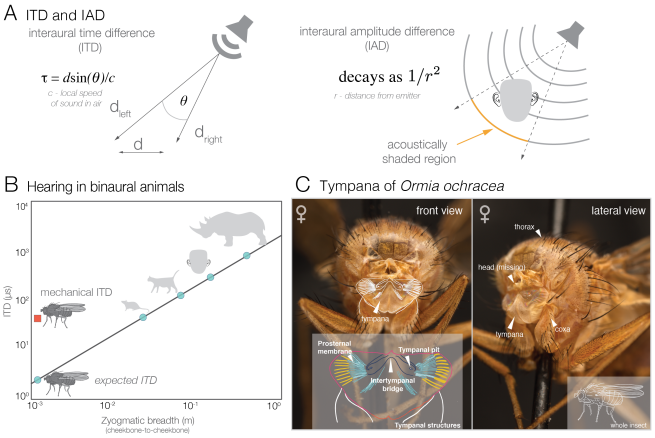

Fig. 1. Hearing in Binaural animals and *Ormia ochracea* (A) ITD and IAD physical meanings. ITD is the delay in time between sound reaching one sensory organ vs the other, defined by the equation $\tau = dsin(\theta)/c$, where d is the distance between the hearing organs and c is the speed of sound in air. IAD is the difference in received amplitude between the left and right sensory organs, due to either acoustic shading or signal decay. **(B)** Chart for approximate ITD values in various animals, calculated using the standard formula defined in (A), with the zyogmatic breadth (cheekbone-to-cheekbone distance) used an approximate measure of interaural distance for mammals and assuming an incident sound angle of 45°. Data obtained from (26–29). **(C)** Female *O. ochracea* post-decapitation, showing location of prosternal membrane, tympanal pits, and intertympanal bridge, all of which were key physical features in the classic 1995 model.

could improve model accuracy and extend the effective range of the model, allowing it to predict more accurate tympanal displacements for incoming sound at high angles when compared to experimental data. In order to identify the sources of inaccuracy in the model, we investigated the detailed physiological structures involved. Using 3D reconstructions of *O. ochracea*'s tympana as a guide, we modified 1995 model by adding terms in order to simulate the mechanics of the hearing organ in the lateral plane. We represent these lateral mechanics mathematically via a spatially-dependent asymmetry in the model spring and damper coefficients. The resulting updated model can be considered quasi-two-dimensional (q2D) and it significantly reduces the average error in mIAD and mITD for large incident sound angles from approximately 60% for mIAD and 15% for mITD, to below 20% in mIAD and below 10% in mITD , in line with the percent error for small incident sound angles in the original 1995 model.

Materials and Methods

Synchrotron x-ray imaging of the ormiine tympana. To better explore the 3D nature of *O. ochracea*'s tympanal physiology, we performed multiaxis x-ray imaging of preserved *O. ochracea* specimens using the synchrotron light source at beamline 2-BM at Argonne National Laboratory. Two *O. ochracea* dried specimens were borrowed from the Virginia Tech Insect Collection. Placed in slender tubes made of kapton, the ventral thorax was imaged using beamline 2-BM, dedicated to microtomography, at Argonne National Laboratory. Each specimen was imaged using the beamline's fast 2D phase contrast imaging, giving stacks of images along the z-axis at intervals of 1.72 microns.

Raw microtomographic images were cropped and downsampled using FIJI (30) and segmented in SlicerMorph, (31) a dynamic imaging extension of 3D Slicer. To segment, features of the tympana were highlighted and then reconstructed in

DRAFT

3D for applicable measurements. A link to the code for the model is available in the Supplemental Material.

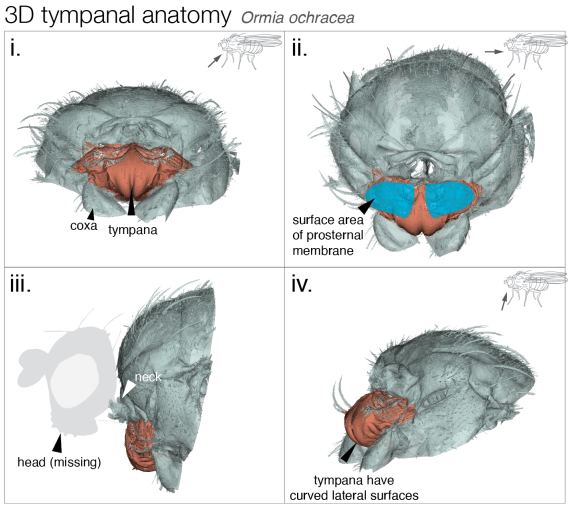

Fig. 2. 3D reconstructions of *O. ochracea* tympanal organs and frontal prothorax. Tympanal membranes highlighted in blue (ii.) with supporting structures highlighted in peach. Orientation of image relative to *O. ochracea* body indicated in top right of i-iv. 3D images made in SlicerMorph (31)

1995 mechanical model. The original mechanical model (11) for the ormiine hearing system treats the tympanal structure as a pair of beams pinned at a central pivot with lumped-mass approximations of the two sides of the hearing organ located at the ends of the beams (Fig. 3A, left). The beams are anchored to the substrate at their distal ends with a pair of symmetric spring-damper elements, and to each each other with a third spring-damper element (Fig. 3A, right). Pressure forces from incident sound waves are applied to the point masses via a forcing function composed of the product of the incident pressure magnitude, the inward-facing unit normal vector, and the tympanal surface area, s (see the Supplement for numerical values used in this study). A time delay is applied between the left and right sides based on the angle θ the incoming sound wave has relative to the midline of the fly, with 0° defined as straight ahead (11).

Previous mathematical model. In addition to the mechanical model described in the previous section, Miles *et al.* developed an accompanying mathematical model (11). Their model is a set of coupled ordinary differential equations that represent the equations of motion for the mechanical model. It treats the incident acoustic pressure acting on the tympanal membranes as two point forces, $f_1(t)$ and $f_2(t)$, acting on the point masses representing the tympanal membranes and associated structures. The dependent variable in the problem is $\mathbf{x}(t)$, which represents the one-dimensional response of each tympanum. The model can be written as:

$$\begin{bmatrix} k_1 + k_3 & k_3 \\ k_3 & k_2 + k_3 \end{bmatrix} \mathbf{x} + \begin{bmatrix} c_1 + c_3 & c_3 \\ c_3 & c_2 + c_3 \end{bmatrix} \dot{\mathbf{x}} + \begin{bmatrix} m & 0 \\ 0 & m \end{bmatrix} \ddot{\mathbf{x}} = \mathbf{f}, \quad [1]$$

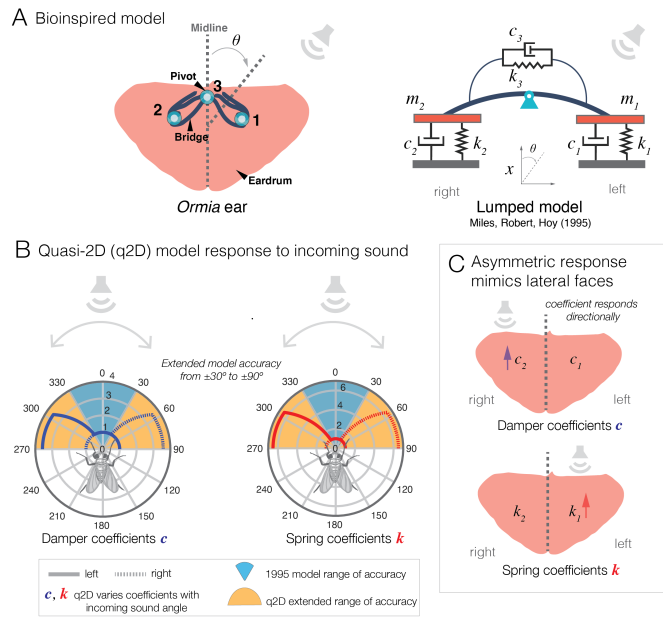

Fig. 3. 1995 model structure, parameters, and q2D model modifications. A) The lumped-parameter mechanical model for hearing in *O. ochracea*. **Left:** Schematic of the coupled tympanal membranes of *O. ochracea* (peach-colored, labeled 1 and 2), connected by the cuticular bridge (blue) with sound incident at θ degrees. **Right:** The hearing system can be represented as a pair of coupled beams joined and anchored by a set of springs and dampers. *Adapted from Liu (2013)(32).* **B)** Model modifications show improved range of accurate model response to incident sound. In the q2D model, normalized damper (red) and spring (blue) coefficients act as a function of incoming sound angle. Improved model responds accurately within $\pm 90°$, compared to $\pm 30°$ of the 1995 model. **C)** q2D model has asymmetric response where the spring/damper coefficients on the same side as the sound source increase as a function of incident sound angle, while the coefficients on the contralateral side remain constant.

$$\mathbf{f} = \begin{bmatrix} f(t) \\ f(t + \delta t) \end{bmatrix} \quad [2]$$

where $\mathbf{x} = (x_1(t), x_2(t))$ is the unknown response vector containing the vertical displacement of the left and rightmost tips of the beams in Figure 3A, which represent the two sides of the intertympanal cuticular bridge, the applied force is $\mathbf{f} = (f_1(t), f_2(t))$, and $\dot{(\ )}$ represents differentiation with respect to time, t. The parameters k_i and c_i are spring stiffness and damper constants, respectively and the parameter m is the effective mass of all the moving parts of the auditory system (11).

q2D model modifications based on ormiine morphology. In Miles *et al.*'s analysis of their 1995 model, the ormiine hearing structure is assumed to be left-right symmetrical and the spring and damper coefficients on the right and left sides are identical and are constant for all incident sound angles, with $k_1 = k_2 = k$ and $c_1 = c_2 = c$, independent of the values of k_3 and c_3.

In order to add a realistic degree of sensitivity to the angle of the incoming sound, we sought to modify the spring and damper parameters in order to incorporate aspects of the 3D morphology of the ormiine hearing organ. We did this by making the magnitude of k and c functions. The functions were designed such that for an incident sound angle above $\pm 30°$, the ipsilateral tympanal response is greater than the

contralateral response, mimicking he presence of lateral sides on the tympana which can both shield the rest of the structure and be more responsive to laterally oriented incoming sounds. Specifically, we provided the following quasi-two-dimensional modification to the 1995 model for ormiine hearing:

$$k(\theta) = \begin{cases} k_0 & \text{if } \theta < |30°| \\ \alpha|\theta|k_0 + \beta & \text{if } |55°| > \theta \geq |30°| \\ k_f & \text{if } \theta \geq |55°| \end{cases} \quad [3]$$

$$\alpha = \frac{k_f - k_0}{25°} \quad [4]$$

$$\beta = \frac{2.6k_0}{25°} \quad [5]$$

where k_0 and k_1 are the minimum and maximum values that the spring stiffness coefficients can take on, respectively. The form of the modified spring coefficient function, two constant segments with a linear ramp between $|30|°$ and $|55|°$ (for a visual representation, see Fig. 3B), was informed by observed lateralization behavior demonstrated by *O. ochracea* (17) and the analysis of an *O. ochracea*-inspired sensor (32). These works indicated the presence of two separate behavioral regimes, a localization regime from 0° to $\leq |30|°$ and a lateralization regime at higher angles. This choice is further supported by the accuracy of the fit to experimental data for sound incident at $\geq |30|°$ (see Fig. 4) and physically represents a degree of elastic response in the lateral direction in response to force from incoming sound waves.

The constants in equations 3-5 were chosen to provide the best fit to previous behavioral data (11): mITD and mIAD derived from laser vibrometer measurements of tympanal membrane vibrations in *O. ochracea* specimens in response to a to 6 kHz sound source as a function of incident sound angle. The coefficients are only modified on the side where the sound source is located, and the coefficients on the contralateral side remain constant. As the incident sound angle approaches ±90° relative to the fly's head, the spring coefficient for the ipsilateral side increases from k_0, approaching k_f according to Equation 3. For example, for sound incident from −30°, the spring and damper coefficients for the left side, k_1 and c_1, would change and k_2 and c_2 would remain unchanged. We assume the total tympanal surface area A is fixed, and we use previously established values (11) throughout this work, $A = 0.288x10^{-6}m^2$. The increases in the spring and damper coefficients, normalized relative to their starting values (k_0), are visible in Figure 3B.

MATLAB's ODE45 function was used to integrate equations 1-2, and a custom peak-finding algorithm was implemented to calculate mITD and mIAD. Further computational details can be found in the Supplemental Material and a link to code samples can be found in the Supplemental Material.

Results

The tympana of *O. ochracea* protrude anteriorly from underneath the fly's head, with distinct lateral faces and sharp curvature (Fig.2). Figure 2 shows 3D surface renderings of *O. ochracea* tympanal membranes in teal, with the supporting structures highlighted in peach. The organs are far from the simple two-dimensional surfaces most often used in the literature (10, 11, 25, 32). These 3D models motivated our modifications to include aspects of actual morphology. The confirmation of significant lateral-facing portions of the tympana led to the modified, q2D model equations 3-5, which account for the lateral tymapanal response to acoustic stimuli.

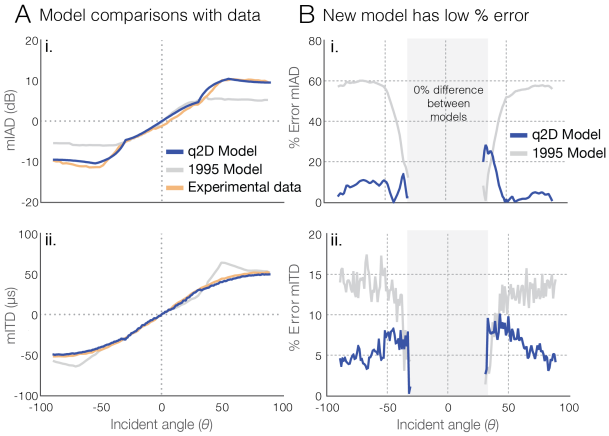

Fig. 4. Comparison between 1995 model, experimental data, and q2D model. Experimental and model results **(A)** and error **(B)** in mITD and mIAD for the standard 1D (1995 model) and q2D models. In **(A)**, mITD and mIAD were calculated from the q2D and 1995 models as a function of incident sound angle for a frequency of 6000 Hz, compared with laser-vibrometry measurements from recently dead *O. ochracea* specimens (11). The significant divergence from behavioral data present in the 1995 model outside ±30°, particularly for mIAD, is rectified in the modified model. In **(B)**, the gray box indicates errors below ±30°, which are not considered because the q2D and 1995 models are identical for these ranges. The errors for the q2D model peak close to ±30°, then decrease as incident sound angle is increased.

Values of mITD and mIAD, calculated from the q2D and 1995 models, are shown in Figure 4 as a function of incident sound angle, and are compared to experimental measurements with recently sacrificed *O. ochracea* specimens (11). Both models are identical for incident sound angles less than ±30°, so the results are identical within that range (Fig. 4B, gray box). When we included the lateral response through the new $k(\theta)$ and $c(\theta)$ functions, the gap between experimental measurements and model results in both mIAD and mITD narrows significantly for 6 kHz signal input (Fig. 4), with the q2D model having average error of approximately 6% and a peak error of approximately 28% in mITD, and an average error of approximately 7% and a peak error of approximately 10% in mIAD. These results additionally confirm that the inclusion of 3D or quasi-2D elements in the model is an important element to the mechanics of ormiine hearing.

Discussion

In this paper, we present the results of 3D X-ray synchrotron imaging of the mechanically-coupled tympana in the parasitoid fly, *Ormia ochracea*, and subsequent modification to the classic model for its hearing inspired by those results. The tympana were confirmed to be highly 3D, with significant lateral-facing membranes, in contrast to the commonly simplified representation of the membranes as flat and front-facing plates.

Detailed knowledge of the hearing organ's morphology allowed us to update the classic 1995 1D model into a quasi-two-dimensional mathematical model for ormiine hearing that added the tympanal response in the lateral direction. Our updated q2D model has significantly improved fidelity to available experimental data (11) compared to the 1995 model,

DRAFT

both in the mechanical interaural time delay (mITD) and in the mechanical interaural amplitude difference (mIAD) (Fig.4B). When compared to the 1995 model, the new q2D model exhibits maximum errors (relative to experimental values) reduced by approximately 50% and 85% respectively. This strongly supports the premise that there are important mechanical aspects to *Ormia* hearing aside from the response of the front-facing tympanal membranes, and that the entirety of the hearing organ structures are sensitive to the angle of incoming sound, a feature that was not included in the 1995 model.

This is one of the first attempts to update the foundational 1995 model for application to *O. ochracea*, and it may be further refined by incorporating additional physiological features of the tympana, such as elastic responses in the membrane, or the ridged elements present surrounding the tympanal membranes. It could also be improved by simple analytic modifications to expand the model's capabilities without impacting its tractability, such as using functions more flexible than simple linear ramps for the spring and damper coefficients. For example, in our q2D model, the "bump" visible near $\pm 45°$ in mIAD in Figure 4A and the uptick at the same point in mITD may be a result of the values for either the springs, dampers, or the ratio between the two, being slightly too high at that point. It is also important to note that this work and the 1995 model both rely on tuning the coefficients so that the model outputs better match the experimental response to sinusoidal input (2 kHz for the 1995 work and 6 kHz for the work here). Although performance was not observed to degrade at other frequencies, the degree of improvement (relative to experimental data) was far less significant than in the 6 kHz input case. The model's poor performance at frequencies other than those tuned specifically for crickets may be resolved by the introduction of other morphological features in the form of frequency-dependent functions, as we have introduced spatially-dependent functions here.

Our model demonstrates that the mechanics of hearing in *O. ochracea* are dependent on the complex tympanal morphology present in the animal, especially with respect to mIAD, and indicates that this morphology serves a specific angle-dependent role in responding to incoming sound waves. The inclusion of angle-dependent behavior in the spring and damper coefficients provides a more accurate understanding of how the insect receives sound. Previous work has demonstrated that *O. ochracea* engages in different behaviors depending on the relative angle of incoming sound (11, 17, 32, 33), with two distinct response patterns. In the first, from 0° to $\pm 30°$, the fly makes relatively narrow adjustments to localize the origin of the sound (localization). In the other, at angles exceeding approximately $\pm 30°$, the fly makes significantly larger adjustments, more akin to determining the side from which the sound originates (lateralization). Our results show that this difference in response is not strictly a result of behavioral differences, but is paired with a difference in physiological responses to incoming sound.

Furthermore, there is growing evidence that some *O. ochracea* are involved in an evolutionary arms race with their host species (34, 35), and that they are capable of differentiating between different cricket host species based on their acoustic signalling, exhibiting preference towards local populations (36). Consequently, the mechanical parameters for the model may depend heavily not only on the geographic origin of *O. ochracea* samples, but also when collection occurred. The degree of tuning to host-searching behavior, as opposed to predator-avoidance behavior, also remains unaddressed experimentally, despite the startle responses when in flight and subjected sound consistent with bat sonar frequencies (5). *O. ochracea* also exhibits a sorting behavior (being able to rapidly categorize sounds as belonging to a predator or not) in response to predator-consistent sound sources, as opposed to host or neutral sound sources. *O. ochracea* is also only one of many *Ormia* species, which parasitize a diverse range hosts, and display different behavioral responses to the acoustic signalling of their hosts (3). Only *O. ochracea* has been examined in sufficient detail to develop a mechanical model with accurate parameters; consequently, it may be worth investigating the mechanics of other ormiine species (3, 37). It may also be worth revisiting the hearing organs in *Emblemasoma*, another group of parasitoid flies, which represent a case of convergent evolution in a distantly related family, *Sarcophagidae* (38, 39).

O. ochracea's hearing system has repeatedly served as a source of inspiration for bio-inspired designs for directional microphones and hearing aids (19–25, 32). Including the angle-dependent behavior of the expanded q2D model in future *Ormia*-inspired device designs may also provide significant avenues for improvement in device performance, or may expand the functionality of devices like acoustic sensors through miniaturization and tunable frequency sensitivities. Currently, work is being undertaken to explore the inclusion of lateral faces on a directional microphone to further study the role that these elements play and attempt to develop a novel practical application. However, there are numerous avenues for exploration remaining, both experimental and theoretical. These include the development of improved bio-inspired technology by incorporating higher-dimensional features and parameter variations in the mechanical system, studying the behavior of the model at frequencies commensurate with bat sonar, and investigating the role that mechanical differences play in *O. ochracea*'s hearing when addressing acoustic preferences. Finally, our expanded q2D model is the first mathematical model for hearing in an binaural fly that is accurate for all measured incident sound angles. It demonstrates the importance of incorporating higher-dimensional model elements consistent with observed physiology, furthering our understanding of binaural and insect hearing.

ACKNOWLEDGMENTS. The authors thank the Virginia Tech Insect Collection for lending the *Ormia ochracea* samples for imaging, and Pavel Shevchenko for assistance in imaging at 2-BM at Argonne National Laboratory. This material is based upon work supported by the National Science Foundation under Grant number 2014181.

1. LROP R.S., Xii. on our perception of sound direction. *The London, Edinburgh, Dublin Philos. Mag. J. Sci.* **13**, 214–232 (1907).
2. WH Cade, Acoustically orienting parasitoids: fly phonotaxis to cricket song. *Science* **190**, 1312–1313 (1975).
3. TJ Walker, Walker, tj phonotaxis in female ormia ochracea (diptera: Tachinidae), a parasitoid of field crickets. *J. Insect Behav.* **6** (1993).
4. D Robert, M Read, R Hoy, The tympanal hearing organ of the parasitoid fly ormia ochracea (diptera, tachinidae, ormiini). *Cell tissue research* **275**, 63–78 (1994).
5. M Rosen, EC Levin, RR Hoy, The cost of assuming the life history of a host: acoustic startle in the parasitoid fly ormia ochracea. *J. Exp. Biol.* **212**, 4056–4064 (2009).
6. DD Yager, Predator detection and evasion by flying insects. *Curr. opinion neurobiology* **22**, 201–207 (2012).
7. N Lee, DO Elias, AC Mason, A precedence effect resolves phantom sound source illusions in the parasitoid fly ormia ochracea. *Proc. Natl. Acad. Sci.* **106**, 6357–6362 (2009).

DRAFT

8. MA Bee, C Micheyl, The cocktail party problem: what is it? how can it be solved? and why should animal behaviorists study it? *J. comparative psychology* **122**, 235 (2008).
9. D Robert, J Amoroso, RR Hoy, The evolutionary convergence of hearing in a parasitoid fly and its cricket host. *Science* **258**, 1135–1137 (1992).
10. M Akcakaya, A Nehorai, Performance analysis of the ormia ochracea's coupled ears. *The J. Acoust. Soc. Am.* **124**, 2100–2105 (2008).
11. RN Miles, D Robert, RR Hoy, Mechanically coupled ears for directional hearing in the parasitoid fly ormia ochracea. *The J. Acoust. Soc. Am.* **98**, 3059–3070 (1995).
12. WH Cade, M Ciceran, AM Murray, Temporal patterns of parasitoid fly (ormia ochracea) attraction to field cricket song (gryllus integer). *Can. J. Zool.* **74**, 393–395 (1996).
13. D Robert, R Miles, R Hoy, Tympanal mechanics in the parasitoid fly ormia ochracea: intertympanal coupling during mechanical vibration. *J. comparative physiology A* **183**, 443–452 (1998).
14. D Robert, U Willi, The histological architecture of the auditory organs in the parasitoid fly ormia ochracea. *Cell tissue research* **301**, 447–457 (2000).
15. ML Oshinsky, RR Hoy, Physiology of the auditory afferents in an acoustic parasitoid fly. *J. Neurosci.* **22**, 7254–7263 (2002).
16. JL van Hemmen, J Christensen-Dalsgaard, CE Carr, PM Narins, Animals and ice: meaning, origin, and diversity (2016).
17. AC Mason, ML Oshinsky, RR Hoy, Hyperacute directional hearing in a microscale auditory system. *Nature* **410**, 686–690 (2001).
18. AC Mason, N Lee, ML Oshinsky, The start of phonotactic walking in the fly ormia ochracea: a kinematic study. *J. Exp. Biol.* **208**, 4699–4708 (2005).
19. R Miles, R Hoy, The development of a biologically-inspired directional microphone for hearing aids. *Audiol. Neurotol.* **11**, 86–94 (2006).
20. R Bauer, et al., Influence of microphone housing on the directional response of piezoelectric mems microphones inspired by ormia ochracea. *IEEE Sensors J.* **17**, 5529–5536 (2017).
21. Y Zhang, et al., A low-frequency dual-band operational microphone mimicking the hearing property of ormia ochracea. *J. Microelectromechanical Syst.* **27**, 667–676 (2018).
22. M Touse, J Sinibaldi, G Karunasiri, Mems directional sound sensor with simultaneous detection of two frequency bands in *SENSORS, 2010 IEEE*. (IEEE), pp. 2422–2425 (2010).
23. C Gibbons, RN Miles, Design of a biomimetic directional microphone diaphragm in *Proceedings of IMECE*. (ASME, State University of New York at Binghamton, Department of Mechanical Engineering), pp. 173–179 (2000).
24. A Rahaman, B Kim, Sound source localization by ormia ochracea inspired low–noise piezoelectric mems directional microphone. *Sci. reports* **10**, 1–10 (2020).
25. R Miles, et al., A low-noise differential microphone inspired by the ears of the parasitoid fly ormia ochracea. *The J. Acoust. Soc. Am.* **125**, 2013–2026 (2009).
26. C Susanne, A Guidotti, R Hauspie, Age changes of skull dimensions. *Anthropol. Anzeiger*, 31–36 (1985).
27. CP Groves, The skulls of asian rhinoceroses: wild and captive. *Zoo Biol.* **1**, 251–261 (1982).
28. DJ Tollin, K Koka, Postnatal development of sound pressure transformations by the head and pinnae of the cat: monaural characteristics. *The J. Acoust. Soc. Am.* **125**, 980–994 (2009).
29. C Katsaros, R Berg, S Kiliaridis, Influence of masticatory muscle function on transverse skull dimensions in the growing rat. *J. Orofac. Orthop. der Kieferorthopädie* **63**, 5–13 (2002).
30. J Schindelin, et al., Fiji: an open-source platform for biological-image analysis. *Nat. methods* **9**, 676–682 (2012).
31. S Rolfe, et al., Slicermorph: An open and extensible platform to retrieve, visualize and analyse 3d morphology. *Methods Ecol. Evol.* **n/a** (year?).
32. H Liu, L Currano, D Gee, T Helms, M Yu, Understanding and mimicking the dual optimality of the fly ear. *Sci. reports* **3**, 1–6 (2013).
33. P Muller, D Robert, A shot in the dark: the silent quest of a free-flying phonotactic fly. *J. Exp. Biol.* **204**, 1039–1052 (2001).
34. M Zuk, JT Rotenberry, RM Tinghitella, Silent night: adaptive disappearance of a sexual signal in a parasitized population of field crickets. *Biol. letters* **2**, 521–524 (2006).
35. S Pascoal, et al., Rapid convergent evolution in wild crickets. *Curr. Biol.* **24**, 1369–1374 (2014).
36. DA Gray, C Banuelos, SE Walker, WH Cade, M Zuk, Behavioural specialization among populations of the acoustically orienting parasitoid fly ormia ochracea utilizing different cricket species as hosts. *Animal Behav.* **73**, 99–104 (2007).
37. T Walker, S Wineriter, Hosts of a phonotactic parasitoid and levels of parasitism (diptera: Tachinidae: Ormia ochracea). *Fla. Entomol.*, 554–559 (1991).
38. R Lakes-Harlan, H Stölting, A Stumpner, Convergent evolution of insect hearing organs from a preadaptive structure. *Proc. Royal Soc. London. Ser. B: Biol. Sci.* **266**, 1161–1167 (1999).
39. D Robert, R Miles, R Hoy, Tympanal hearing in the sarcophagid parasitoid fly emblemasoma sp.: the biomechanics of directional hearing. *J. Exp. biology* **202**, 1865–1876 (1999).

Abbreviations

The following abbreviations are used in this manuscript:

ITD	Interaural Time Delay
IAD	Interaural Amplitude Difference (sometimes called the Interaural Intensity Difference (IID) or Interaural Level Difference (ILD))
mITD	Mechanical Interaural Time Delay
mIAD	Mechanical Interaural Amplitude Difference

DRAFT